Med Bio Eng Comput (2006) 44:1031–1051
DOI 10.1007/s11517-006-0119-0

REVIEW ARTICLE

Heart rate variability: a review

U. Rajendra Acharya · K. Paul Joseph · N. Kannathal · Choo Min Lim · Jasjit S. Suri

Received: 19 October 2005 / Accepted: 10 October 2006 / Published online: 17 November 2006

Abstract Heart rate variability (HRV) is a reliable reflection of the many physiological factors modulating the normal rhythm of the heart. In fact, they provide a powerful means of observing the interplay between the sympathetic and parasympathetic nervous systems. It shows that the structure generating the signal is not only simply linear, but also involves nonlinear contributions. Heart rate (HR) is a nonstationary signal; its variation may contain indicators of current disease, or warnings about impending cardiac diseases. The indicators may be present at all times or may occur at random—during certain intervals of the day. It is strenuous and time consuming to study and pinpoint abnormalities in voluminous data collected over several hours. Hence, HR variation analysis (instantaneous HR against time axis) has become a popular noninvasive tool for assessing the activities of the autonomic nervous system. Computer based analytical tools for in-depth study of data over daylong intervals can be very useful in diagnostics. Therefore, the HRV signal parameters, extracted and analyzed using computers, are highly useful in diagnostics. In this paper, we have discussed the various applications of HRV and different linear, frequency domain, wavelet domain, nonlinear techniques used for the analysis of the HRV.

Keywords Heart rate variability · Autonomic nervous system · Poincare plot · Surrogate data · ANOVA test · Phase space plot · Correlation dimension · Lyapunov exponent · Approximate entropy · Sample entropy · Hurst exponent · Wavelet transform · Recurrent plot

U. Rajendra Acharya (✉) · N. Kannathal · C. M. Lim
Department of ECE, Ngee Ann Polytechnic,
535 Clementi Road, Singapore, Singapore 599 489
e-mail: aru@np.edu.sg

K. Paul Joseph
Electrical Engineering, National Institute of Technology
Calicut, Calilcut 673601 Kerala, India

J. S. Suri
Idaho's Biomedical Research Institute, ID, USA

J. S. Suri
Biomedical Technologies Inc., Westminster, CO, USA

1 Introduction

Heart rate variability (HRV), the variation over time of the period between consecutive heartbeats, is predominantly dependent on the extrinsic regulation of the heart rate (HR). HRV is thought to reflect the heart's ability to adapt to changing circumstances by detecting and quickly responding to unpredictable stimuli. HRV analysis is the ability to assess overall cardiac health and the state of the autonomic nervous system (ANS) responsible for regulating cardiac activity.

HRV is a useful signal for understanding the status of the ANS. HRV refers to the variations in the beat intervals or correspondingly in the instantaneous HR. The normal variability in HR is due to autonomic neural regulation of the heart and the circulatory system [111]. The balancing action of the sympathetic nervous system (SNS) and parasympathetic nervous system (PNS) branches of the ANS controls the HR. Increased SNS or diminished PNS activity results in cardio-acceleration. Conversely, a low SNS activity or a high PNS activity causes cardio-deceleration. The degree of variability in the HR provides information

about the functioning of the nervous control on the HR and the heart's ability to respond.

Past 20 years have witnessed the recognition of the significant relationship between ANS and cardiovascular mortality including sudden death due to cardiac arrest [69, 115, 120]. Numerous numbers of papers appeared in connection with HRV related cardiological issues [8, 13, 57, 58, 64, 87, 97, 112] reiterates the significance of HRV in assessing the cardiac heath. The interest in the analysis of HRV (i.e., the fluctuations of the heart beating in time,) is not new. Furthermore, much progress was achieved in this field with the advent of low cost computers with massive computational power, which fueled many recent advances.

Tulen and Man in t'veld [125] have found that, HR, diastolic blood pressure (BP), mid-frequency band power of HR and systolic BP, and plasma adrenaline concentrations showed significant increase when changed from supine to sitting to standing posture. Viktor et al. [132] have studied the variation of HR spectrogram and breathing rates in lateral and supine body positions. Recently, new dynamic methods of HRV quantification have been used to uncover nonlinear fluctuations in HR, that are not otherwise apparent. Several methods have been proposed: Lyapunov exponents [105], $1/f$ slope [64], approximate entropy (ApEn) [93] and detrended fluctuation analysis (DFA) [91].

Heart rate variability, i.e., the amount of HR fluctuations around the mean HR, can be used as a mirror of the cardiorespiratory control system. It is a valuable tool to investigate the sympathetic and parasympathetic function of the ANS. The most important application of HRV analysis is the surveillance of postinfarction and diabetic patients. HRV gives information about the sympathetic-parasympathetic autonomic balance and thus about the risk for sudden cardiac death (SCD) in these patients. HRV measurements are easy to perform, noninvasive, and have good reproducibility, if used under standardized conditions [46, 63].

Kovatchev et al. [65] have introduced the sample asymmetry analysis (SAA) and illustrate its utility for assessment of HR characteristics occurring, early in the course of neonatal sepsis and systemic inflammatory response syndrome (SIRS). Compared with healthy infants, infants who experienced sepsis had similar sample asymmetry in health, and elevated values before sepsis and SIRS ($p = 0.002$). Cysarz et al. [29] have demonstrated that the binary symbolization of RR interval dynamics, which at first glance seems to be an enormous waste of information, gives an important key to a better understanding of normal heart period regularity. Furthermore, differential binary symbolization still enables the identification of nonlinear dynamical properties.

Recently, Verlinde et al. [129] have compared the HRV of aerobic athletes with the controls and showed that the aerobic athletes have an increased power in all frequency bands. These results are in accordance with values obtained by spectral analysis using the Fourier transform, suggesting that wavelet analysis could be an appropriate tool to evaluate oscillating components in HRV. But, in addition to classic methods, it also gives a time resolution. Time-dependent spectral analysis of HRV using the wavelet transform was found to be valuable for explaining the patterns of cardiac rate control during reperfusion. In addition, examination of the entire record revealed epochs of markedly diminished HRV in two patients, which attribute to vagal saturation [123]. A method for analyzing HRV signals using the wavelet transform was applied to obtain a time-scale representation for very low-frequency (VLF), low-frequency (LF) and high-frequency (HF) bands using the orthogonal multiresolution pyramidal algorithm [44]. Results suggest that wavelet analysis provides useful information for the assessment of dynamic changes and patterns of HRV during myocardial ischaemia. Time-frequency parameters calculated using wavelet transform and extracted from the nocturnal heart period analysis appeared as powerful tools for obstructive sleep apnoea syndrome diagnosis [104]. Time-frequency domain analysis of the nocturnal HRV using wavelet decomposition could represent an efficient marker of obstructive sleep apnoea syndrome [104]. Its added ease of use and interpretation is of interest in considering the high prevalence of sleep-related breathing disorders in a general middle-aged, at-risk population. Recently, Schumacher et al. [114] have explained the use of linear and nonlinear analysis in the analysis of the HR signals. The affect of ANS, BP, myocardial infarction (MI), nervous system, age, gender, drugs, diabetes, renal failure, smoking, alcohol, sleep on the HRV are discussed in detail.

Power spectral analysis of beat-to-beat HRV has provided a useful means of understanding the interplay between autonomic and cardiovascular functionality. Mager et al. [73] have developed an algorithm that utilizes continuous wavelet transform (CWT) parameters as inputs to Kohonen's self-organizing map (SOM), for providing a method of clustering subjects with similar wavelet transform signatures . Bracic et al. [18] have analyzed human blood flow in the time-frequency domain, and used the wavelet transform (Morlet) which gives good time resolution for high frequency components and good frequency resolution

for LF components . Recently, HR (using Morlet wavelet as mother wavelet) for different cardiac arrhythmias was proposed (Oliver et al. 2004). Shimojima et al. [118] have used Morlet mother wavelet to evaluate the performance of frequency power spectrum during QRS in intraventricular conduction abnormalities (IVCA). They have observed that there is reduction of the low frequency power in IVCA and the increased power and number of peaks in high frequency range in IVCA with MI.

1.1 The autonomic nervous system

The ANS have sympathetic and parasympathetic components. Sympathetic stimulation, occurring in response to stress, exercise and heart disease, causes an increase in HR by increasing the firing rate of pacemaker cells in the heart's sino-atrial node. Parasympathetic activity, primarily resulting from the function of internal organs, trauma, allergic reactions and the inhalation of irritants, decreases the firing rate of pacemaker cells and the HR, providing a regulatory balance in physiological autonomic function. The separate rhythmic contributions from sympathetic and parasympathetic autonomic activity modulate the heart rate (RR) intervals of the QRS complex in the electrocardiogram (ECG), at distinct frequencies. Sympathetic activity is associated with the low frequency range (0.04–0.15 Hz) while parasympathetic activity is associated with the higher frequency range (0.15–0.4 Hz) of modulation frequencies of the HR. This difference in frequency ranges allows HRV analysis to separate sympathetic and parasympathetic contributions evident. This should enable preventive intervention at an early stage when it is most beneficial.

1.2 HRV and blood pressure

Several structural and functional alterations of the cardiovascular system that are frequently found in hypertensive individuals may increase their cardiovascular risk beyond that induced by the BP elevation alone. Electrocardiographic evidence of left ventricular hypertrophy (LVH) and strain are associated with increased morbidity and mortality. HRV is significantly reduced in patients with LVH secondary to hypertension or aortic valve disease. Cardiac vagal nerve activity is influenced by the arterial baroreflex. The amplitude of respiratory sinus arrhythmia (HRV) has been found to correlate with baroreflex sensitivity which is reduced in hypertension and diabetes. This reduction in baroreflex sensitivity is correlated with cardiac LVH.

A method to describe relationships between short-term BP fluctuations and heart-rate variability in resting subjects was analyzed in the frequency domain [9, 14–16]. Relationships between pressure and interval variability indicate that the 10-s variability, which indicate in systolic pressure, leads the interval variation by two to three beats and manifest in cross-spectra. However no such lag is found between the respiration-linked variations in systolic pressure. And later they [14–16] have proposed a simple model to interpret the results of spectral analysis of BP and HR data. The baroreflex equation of the model describe the data only in the region of respiratory frequencies. The shape of the phase spectrum of systolic pressures against intervals was modeled by difference equations. But no physiological interpretation of these equations was given. They have proved that, the spectral properties of the input signal can not be recovered fully from the interval spectrum, nor from the spectrum of counts, the more so as physiological series of events were not be generated by an ideal integrated pulse frequency modulation (IPFM) model [14–16]. Recently, the European Society of Hypertension working group on baroreflex and cardiovascular variability, in which 11 centres participated, has produced a comprehensive database which is available for testing and comparison of methods [66]. Recently, Westerhof et al. [137] have proposed a cross-correlation baro-flex sensitivity (xBRS) technique for the computation of time-domain baroreflex sensitivity on spontaneous BP and HRV using EUROBAVAR data set. They proved that, the xBRS method may be considered for experimental and clinical use, because the values yielded were correlated strongly with and was close to the EUROBAVAR averages.

1.3 HRV and myocardial infarction

A predominance of sympathetic activity and reduction in parasympathetic cardiac control has been found in patients with acute MI [108]. Sympathetic activity decreases the fibrillation threshold and predisposes to ventricular fibrillation (VF). Vagal activity increases the threshold and appears to protect against malignant ventricular tachyarrhythmias [117, 138]. The degree of respiratory sinus arrhythmia shows a linear relation with parasympathetic cardiac control [61, 75] and thus can be used as a prognostic tool in patients, who have had a MI. It was shown that, the HRV decreases with the recent MI [21, 22]. Despite the beneficial effects on clinical variables, exercise training did not markedly alter HRV indexes in subjects after MI [32]. A significant decrease in SDRR and HF power in the control

group suggested an ongoing process of sympathovagal imbalance in favor of sympathetic dominance in untrained patients after MI with new-onset left ventricular dysfunction.

1.4 HRV and nervous system

Disorders of the central and peripheral nervous system have effects on HRV. The vagally and sympathetically mediated fluctuations in HR may be independently affected by some disorders. All normal cyclic changes in HR are reduced in the presence of severe brain damage [71] and depression [21, 22]. HRV was less accurate than the Glasgow Coma Scale in predicting outcome. But it was easily accessible and may provide information about the patient's neurologic status [67]. In serial determinations, the rate of return of normal HRV may reflect the subsequent state of neuronal function.

The significance of HRV analysis in psychiatric disorders arises from the fact that one can easily detect a sympatho-vagal imbalance (relative cholinergic and adrenergic modulation of HRV), if it exists in such pathologies. There is conflicting reports about the HRV and the major depression. It is proved that, in physically healthy depressed adults the HRV does not vary from healthy subjects [113].

1.5 HRV and cardiac arrhythmia

A complex system like cardiovascular system cannot be linear in nature and by considering it as a nonlinear system, can lead to better understanding of the system dynamics. Recent studies have also stressed the importance of nonlinear techniques to study HRV in issues related to both health and disease. The progress made in the field using measures of chaos has attracted the scientific community to apply these tools in studying physiological systems, and HRV is no exception. There have been several methods of estimating invariants from nonlinear dynamical systems being reported in the literature. Recently, Fell et al. [39] and Radhakrishna et al. [99] have tried the nonlinear analysis of ECG and HRV signals, respectively. Also, Paul et al. (2002) showed that coordinated mechanical activity in the heart during VF may be made visible in the surface ECG using wavelet transform. Owis et al. [86] have used nonlinear dynamical modeling in ECG arrhythmia detection and classification. Acharya et al. [1–4] have classified the HRV signals using nonlinear techniques, and artificial intelligence into different groups. Dingfie et al. [46] have classified cardiac arrhythmia into six classes using autoregressive (AR) modeling.

1.6 HRV in diabetes

Diabetes can cause severe autonomic dysfunction and can be responsible for several disabling symptoms, including SCD. Although traditional measures of autonomic function are able to document the presence of neuropathy, in general they are only abnormal when there is severe symptomatology. Thus by the time changes in function were evident, the natural course of autonomic neuropathy was well established. HRV and SCD Ventricular tachyarrhythmias represent a leading cause of SCD in the community.

The pathophysiology of SCD was probably an interaction between an abnormal anatomical substrate such as coronary artery disease with associated myocardial scarring, LVH or cardiomyopathy, and transient functional disturbances which trigger the terminal dysrhythmia. This may include factors such as ischaemia, premature beats, electrolyte disturbance and fluctuations in autonomic balance.

The decreased beat-to-beat variability during deep breathing in diabetic neuropathy was first reported by Wheeler and Watkins [139] and confirmed by many others [92]. In studies comparing cardiac autonomic function tests and HRV indices (based on both short (5-min) and 24-h ECG recordings), show that, in diabetic patients without abnormal function tests, HRV was lowered [92]. It was concluded that cardiac (parasympathetic) autonomic activity was diminished in diabetic patients before clinical symptoms of neuropathy become evident [92, 119, 134].

1.7 HRV and renal failure

In patients with renal failure, autonomic function tests have been done [37, 146], followed by HRV indices [41] and spectral analysis of HR [10]. Although autonomic function tests revealed predominant impairment of the PNS [146], spectral analysis exhibited a strong reduction in the HR power spectrum at all frequency ranges, both sympathetically and parasympathetically [10]. The relationship between HRV parameters and electrolyte ion concentrations in both pre- and post-dialysis [124]. The 5-min HRV of 20 chronic renal failure (CRF) patients were analyzed. Results revealed that calcium is negatively correlated to the mean of RR intervals and normalized HF power after hemodialysis. A model of baroreflex control of BP was proposed in terms of a delay differential equation and was used to predict the adaptation of short-term cardiovascular control in CRF patients [68]. They showed that in CRF patients, the mean power in the LF band was higher and lower in the

HF bands than the corresponding values in the healthy subjects.

1.8 HRV and gender, age

It is proved that, the HRV depends on the age and sex also. The HRV was more in the physically active young and old women [30, 110]. It was proved by Emese et al. [80] that the alert new borns have lower HR variation in the boys than in the case of girls. The HR variation for healthy subjects from 20 to 70 years was studied by Bonnemeir et al. 17 and found that the HRV decreases with age and variation is more in the case of female than men.

Previous studies have assessed gender and age-related differences in time and frequency domain indices [100] and some nonlinear component of HRV. There also seemed to be a significant difference between day and night hours when studying HRV indices using spectral and time domain methods [100, 144].

The amount of HRV is influenced by physiologic and maturational factors. Maturation of the sympathetic and vagal divisions of the ANS results in an increase in HRV with gestational age [128] and during early postnatal life [128]. HRV decreases with age [3, 4]. This decline starts in childhood [116]. Infants have a high sympathetic activity that decreases quickly between ages 5 and 10 years [40]. The influence of provocation on HRV (i.e., standing and fixed breathing) is more pronounced at younger ages [116]. In adults, an attenuation of respiratory sinus arrhythmia with advancing age usually predominates [70, 135]. It was shown that compared to men, women are at lower risk of coronary heart disease [140].

1.9 HRV and drugs

Heart rate variability can be significantly influenced by various groups of drugs. The influence of medication should be considered, while interpreting HRV. On the other hand, HRV can be used to quantify the effects of certain drugs on the ANS.

The effects of beta-blockers and calcium channel blockers on the heart rate variability have been studied in postinfarction and hypertensive patients [12, 28, 51]. With spectral analysis, it is possible to unravel the sympathetic and parasympathetic activities of these drugs and thus explain their protective effects in cardiac diseases. In normotensive adults, the beta-adrenergic blocker atenolol appears to augment vagally mediated fast fluctuations in HR [79]. Guzzetti et al. [51] studied the effect of atenolol in patients with essential hypertension. They found not only an increase in HF fluctuations, but also a decrease in the sympathetically mediated LF oscillations. This decrease in sympathetic activity was also noticed in postinfarction patients using metoprolol [12] and in patients with heart failure using acebutolol [28]. Thus, beta-blockers are able to restore the sympathetic–parasympathetic balance in cardiovascular disease. Effect of Omacor on HRV parameters in patients with recent uncomplicated MI was studied [88]. And the study, quantify improvement in time domain HRV indices and can assess the safety of administering Omacor to optimally treated post-infarction patients. Eryonucu et al. [36] have investigated the effects of $ß_2$ -adrenergic agonist therapy on HRV in adult asthmatic patients by using frequency domain measures of HRV. The LF and LF/HF ratio increased and TP decreased at 5, 10, 15 and 20 min after the salbutamol and the terbutaline inhalation, HF will not change significantly after the salbutamol and terbutaline inhalation.

1.10 HRV and smoking

Studies have shown that smokers have increased sympathetic and reduced vagal activity as measured by HRV analysis. Smoking reduces the HRV. One of the mechanisms by which smoking impairs the cardiovascular function is its effect on ANS control [52, 72, 83]. Altered cardiac autonomic function, assessed by decrements in HRV, is associated with acute exposure to environmental tobacco smoke (ETS) and may be part of the pathophysiologic mechanisms linking ETS exposure and increased cardiac vulnerability [98]. Recently Zeskind and Gingras [145] have shown that cigarette exposed fetuses have lower HRV and disrupted temporal organization of autonomic regulation before effects of parturition, postnatal adaptation, and possible nicotine withdrawal contributed to differences in infant neurobehavioral function. Also, it was proved that, the vagal modulation of the heart had blunted in heavy smokers, particularly during a parasympathetic maneuver. Blunted autonomic control of the heart may partly be associated with adverse event attributed to cigarette smoking [11].

1.11 HRV and alcohol

HRV reduces with the acute ingestion of alcohol, suggesting sympathetic activation and/or parasympathetic withdrawal. Malpas et al. [76] have demonstrated vagal neuropathy in men with chronic alcohol dependence using 24 h HRV analysis.

Ryan et al. [109] have previously reported a strong positive association between average day time and

nighttime HR measured during 24 h ambulatory BP monitoring and usual alcohol intake. ECG indices of vagal activity have been reported to have significantly lower indices of cardiac vagal nerve activity than normal volunteers, in acute alcoholic subjects [76, 90, 106].

1.12 HRV and sleep

The results from Togo and Yamamoto [122] suggest that mechanisms involving electroencephalographic desynchronization and/or conscious states of the brain are reflected in the fractal component of HRV. Compared to stages 2 and 4 non-REM sleep, the total spectrum power was significantly higher in REM sleep and its value gradually increased in the course of each REM cycle [20]. The value of the VLF component (reflects slow regulatory mechanisms, e.g., the renin-angiotensin system, thermoregulation) was significantly higher in REM sleep than in stages 2 and 4 of non-REM sleep. The LF spectral component (linked to the sympathetic modulation) was significantly higher in REM sleep than in stages 2 and 4 non-REM sleep. Patients with sleep apnoea tend to have a spectral peak lying between 0.01 and 0.05cycles/beat, with the width of the peak indicating variability in the recurrence rate of the apnoea. In most of the subjects, the frequency spectrum immediately below the apnoea peak was relatively flat. The first visual analysis of the single computed spectrum from each subject led to a correct classification score of 28/30 (93%) [31]. Gates et al. [45] suggested that, a long-lasting alterations existed in autonomic function in snoring subjects.

1.13 In infants

Investigations in the fetus and newborn have revealed that, during rapid eye movement (REM) sleep long-term variability (LTV) was increased and short-term variability (STV) decreased compared to during non-REM sleep [107, 128]. These differences between REM and non-REM sleep, were due to a shift in the vagal-sympathetic balance from a higher sympathetic tone during REM sleep to a higher vagal tone during non-REM sleep [127]. In addition, the slower and more regular breathing in non-REM sleep (more respiratory sinus arrhythmia, thus more STV) contributes to the differences found. Higher HR and lower total power lower was found in infants than in children [133]. It was proved that, during the deep sleep, the HRV decreases in healthy subjects [34]. HF power was higher in children than in infants. In infants and children, the ratio between LF and HF powers changed with the various sleep stages ($p < 0.02$ in infants; $p < 0.01$ in children): it decreased during deep sleep and increased during REM sleep.

Heart rate variability is a measure of variations in the HR. Figure 1 shows the variation of the HR of a normal subject. It is usually calculated by analyzing the time series of beat-to-beat intervals from ECG or arterial pressure tracings. Various measures of HRV have been proposed, which can roughly be subdivided into time domain, frequency domain and nonlinear domain measures.

2 Methods

2.1 Time domain analysis

Two types of HRV indices are distinguished in time domain analysis. Beat-to-beat or STV indices represent fast changes in HR. LTV indices are slower fluctuations (fewer than 6 min^{-1}). Both types of indices are calculated from the RR intervals occurring in a chosen time window (usually between 0.5 and 5 min). From the original RR intervals, a number of parameters are calculated: SDNN, the standard deviation of the NN intervals, SENN is the standard error, or standard error of the mean, is an estimate of the standard deviation of the sampling distribution of means, based on the data, SDSD is the standard deviation of differences between adjacent NN intervals. RMSSD, the root mean square successive difference of intervals, pNN50%, the number of successive difference of intervals which differ by more than 50 ms expressed as a percentage of the total number of ECG cycles analyzed. The statistical parameters SDNN, SENN, SDSD, RMSSD, NN50 (%), and pNN50% [120] can be used as time domain parameters.

The statistical parameters SDNN, SENN, SDSD, RMSSD, pNN50% and TINN are found to have bigger value for the classes like preventricular contraction

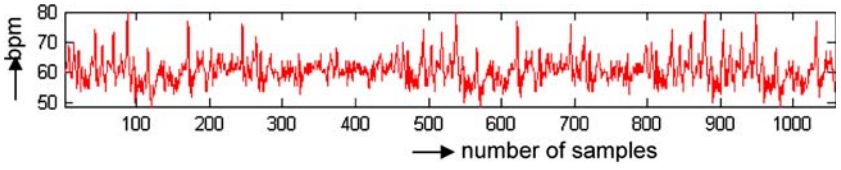

Fig. 1 Heart rate variation of a normal subject

(PVC), sick sinus syndrome (SSS), and atrial fibrillation (AF) due to higher RR variation. And for the slowly varying signal like complete heart block (CHB), left bundle branch block (LBBB) and Ischemic/dilated cardiomyopathy, these parameters will be lesser because of the smaller RR variation [1, 3].

2.1.1 Analysis by geometrical method

Geometrical methods present RR intervals in geometric patterns and various approaches have been used to derive measures of HRV from them. The triangular index is a measure, where the length of RR intervals serves as the x-axis of the plot and the number of each RR interval length serves as the y-axis. The length of the base of the triangle is used and approximated by the main peak of the RR interval frequency distribution diagram. The triangular interpolation of NN interval histogram (TINN) is the baseline width of the distribution measured as a base of a triangle, approximating the NN interval distribution (the minimum of HRV). Triangular interpolation approximates the RR interval distribution by a linear function and the baseline width of this approximation triangle is used as a measure of the HRV index [38, 74]. This triangular index had a high correlation with the standard deviation of all RR intervals. But it is highly insensitive to artifacts and ectopic beats, because they are left outside the triangle. This reduces the need for preprocessing of the recorded data [74]. The major advantage of geometric methods lies in their relative insensitivity to the analytical quality of the series of NN intervals. The typical values of different statistical and geometric parameters of HR signal (Fig. 1) is shown in Table 1.

Table 1 Result of statistical and geometric parameters of heart rate (Fig. 1)

Time domain statistics		
Variable	Units	Value
Statistical measures		
SDNN	ms	30.0
SENN	ms	4.12
SDSD	ms	36.6
RMSSD	ms	33.3
NN50	Count	0
pNN50	%	0.0
Geometric measures		
RR triangular index		0.011
TINN	ms	20.0

2.1.2 Poincare geometry

The Poincare plot, is a technique taken from nonlinear dynamics and portrays the nature of RR interval fluctuations. It is a plot in which each RR interval plotted as a function of the previous RR interval. Poincare plot analysis is an emerging quantitative-visual technique, whereby the shape of the plot is categorized into functional classes, that indicate the degree of the heart failure in a subject [143]. The plot provides summary information as well as detailed beat-to-beat information on the behavior of the heart [59]. This plot may be analyzed quantitatively by calculating the standard deviations of the distances of the R–$R(i)$ to the lines $y = x$ and $y = -x + 2R$–R_m, where R–R_m is the mean of all R–$R(i)$ [126]. The standard deviations are referred to as SD1 and SD2, respectively. SD1 related to the fast beat-to-beat variability in the data, while SD2 describes the longer-term variability of R–$R(i)$ [126]. The ratio SD1/SD2 may also be computed to describe the relationship between these components. Figure 2 shows the Poincare plot of a normal subject (shown in Fig. 1).

SD1/SD2 shows the ratio of short interval variation to the long interval variation. This ratio is more in the case of PVC, AF, SSS and VF due to more variation in the RR interval. But, this ratio falls (below normal) for the slowly varying signals like CHB, Ischemic/dilated cardiomyopathy [3, 4].

2.2 Frquency domain analysis

The time domain methods are computationally simple, but lack the ability to discriminate between sympathetic and para-sympathetic contributions of HRV. These studies of HRV employed the periodogram or fast Fourier transform (FFT) for power spectral density (PSD) estimation procedure consists of two steps. Given the data sequence $x(n)$, $0 \leq n \leq N$–1, the parameters of the method are estimated. Then from these estimates, the PSD estimate is computed. But these methods suffer from spectral leakage effects due to windowing. The spectral leakage leads to masking of weak signal that are present in the data. The parametric (model based) power spectrum estimation methods avoid the problem of leakage and provide better frequency resolution than nonparametric or classical method. AR method can be used for the analysis of frequency domain.

In AR method, the estimation of AR parameters can be done easily by solving linear equations. In AR method, data can be modeled as output of a causal, all pole, discrete filter whose input is white noise.

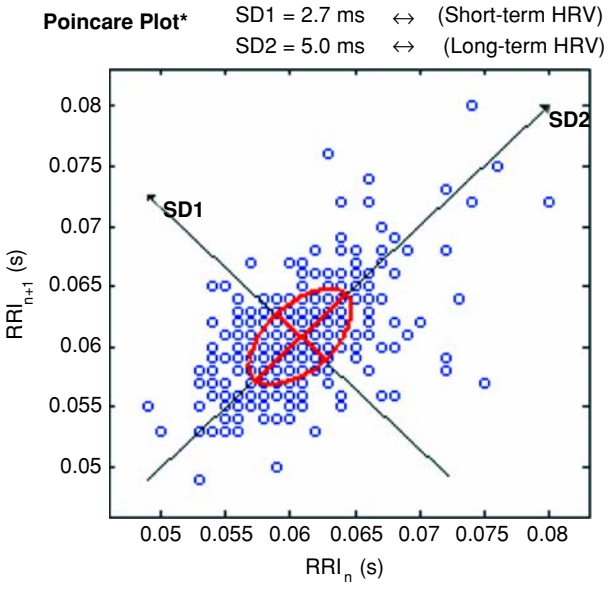

Fig. 2 Poincare plot of a normal subject (shown in Fig. 1)

AR method of order p is expressed as the following equation:

$$x(n) = -\sum_{k=1}^{p} a(k)x(n-k) + w(n) \tag{1}$$

where $a(k)$ are AR coefficients and $w(n)$ is white noise of variance equal to σ^2. AR (p) model can be characterized by AR parameters $\{a[1], a[2],..., a[p], \sigma^2\}$.

The important aspect of the use of AR method, is the selection of the order p. Much work has been done by various researchers on this problem and many experimental results have been given in literature such as the papers presented by Akaike [5, 6, 19]. The order of the AR model $p = 16$ can be taken [19].

An AR process, $x(n)$, may be represented as the output of an all-pole filter, i.e., driven by unit variance white noise. The Burg method is used to get the AR model parameter. The power spectrum of a p th order AR process is

$$P_{xx}^{\mathrm{BU}}(f) = \frac{\hat{\bar{E}}_p}{\left|1 + \sum_{k=1}^{p} \hat{a}_p(k)\, \mathrm{e}^{-j2\pi fk}\right|^2} \tag{2}$$

where $\hat{\bar{E}}$ is total least square error. The Burg method results in high resolution and yields a stable AR model.

Spectral analysis of HRV can be a powerful tool to assess ANS function. It is not only useful when studying the pathophysiologic processes in certain diseases but also may be used in daily clinical practice. Figure 3 indicates the AR spectrum of a normal subject (shown in Fig. 1).

In the frequency domain, ratio of low frequency to the high frequency is high for the CHB and Ischemic/dilated cardiomyopathy abnormalities are high, because the RR variation is very small. This RR variation will be more (as compared to the normal) in the case of LBBB, AF, SSS, PVC and VF. Hence, this ratio will be more. So, for the abnormal cases, this ratio either decreases or increases from the normal range [3, 4]. The typical values of different frequency domain parameters of HR signal (Fig. 1) is shown in Table 2.

2.2.1 *Limitations of Fourier analysis*

Conventional signal methods of analysis based on Fourier transform technique are not very suitable for analyzing nonstationary signals. The Fourier transform technique resolves the time domain signal into complex exponential functions, along with information of their phase shift measured with respect to a specific reference instant. Here the frequency components extend from $-\infty$ to $+\infty$ in the time scale. That is, even finite length signals are expressed as the sum of frequency components of infinite duration. Besides, the phase angle being a modular measure, it fails to provide the exact location of an 'event' along the time scale. This is a major limitation of the Fourier transform approach.

2.2.2 *Higher order spectra*

The HRV signal can be analyzed using different higher order spectra (HOS) (also known as polyspectra) that are spectral representations of higher order moments or cumulants of a signal. The Bispectrum is the Fourier Transform of the third order correlation of the signal and is given by

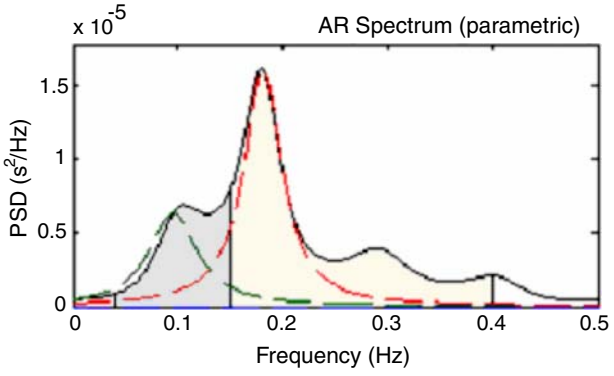

Fig. 3 AR spectrum of heart rate signal shown in Fig. 1

Table 2 Result of frequency domain parameters of heart rate signal (Fig. 1)

Frequency band	Peak (Hz)	Power (ms^2)	Power (%)	Power (n.u.)
VLF	0.0000	0	0.0	
LF	0.0957	0	29.7	13.6
HF	0.0957	1	70.3	32.3
LF/HF	0.1816		0.422	

$$B(f_1,f_2) = E[X(f_1) \times (f_2)X*(f_1+f_2)] \tag{3}$$

where $X(f)$ is the Fourier transform of the signal $x(nT)$ and $E[.]$ stands for the expectation operation. In practice, the expectation operation is replaced by an estimate that is an average over an ensemble of realizations of a random signal. For deterministic signals, the relationship holds without an expectation operation with the third order correlation being a time-average. For deterministic sampled signals, $X(f)$ is the discrete-time Fourier transform and in practice is computed as the discrete Fourier transform (DFT) at frequency samples using the FFT algorithm. The frequency f may be normalized by the Nyquist frequency to be between 0 and 1.

The bispectrum may be normalized (by power spectra at component frequencies) such that it has a value between 0 and 1, and indicates the degree of phase coupling between frequency components [84]. The normalized bispectrum or bicoherence is given by

$$B_{\mathrm{co}}(f_1,f_2) = \frac{E(X(f_1)X(f_2)X*(f_1+f_2)]}{P(f_1)P(f_2)P*(f_1+f_2)} \tag{4}$$

where $P(f)$ is the power spectrum.

2.2.2.1 Higher order spectral features One set of features are based on the phases of the integrated bispectrum derived by Chandran et al. [24] and is described briefly below.

Assuming that there is no bispectral aliasing, the bispectrum of a real signal is uniquely defined with the triangle $0 \le f_2 \le f_1 \le f_1 + f_2 \le 1$. Parameters are obtained by integrating along the straight lines passing through the origin in bifrequency space. The region of computation and the line of integration are depicted in Fig. 4. The bispectral invariant, $P(a)$, is the phase of the integrated bispectrum along the radial line with the slope equal to a. This is defined by

$$P(a) = \arctan\left(\frac{I_{\mathrm{i}}(a)}{I_{\mathrm{r}}(a)}\right) \tag{5}$$

where

$$I(a) = I_{\mathrm{r}}(a) + jI_{\mathrm{i}}(a) = \int_{f_1=0^+}^{\frac{1}{1+a}} B(f_1, af_1)\,\mathrm{d}f_1 \tag{6}$$

for $0<a \le 1$, and $j = \sqrt{-1}$. The variables I_r and I_i refer to the real and imaginary part of the integrated bispectrum, respectively.

These bispectral invariants contain information about the shape of the waveform within the window and are invariant to shift and amplification and robust to time-scale changes. They are particularly sensitive to changes in the left–right asymmetry of the waveform. For windowed segments of a white Gaussian random process, these features will tend to be distributed symmetrically and uniformly about zero in the interval $[-\pi, +\pi]$. If the process is chaotic and exhibits a colored spectrum with third order time-correlations or phase coupling between Fourier components, the mean value and the distribution of the invariant feature may be used to identify the process.

Another set of features are based on the work of Ng et al. [82]. These features are the mean magnitude and the phase entropy. However, unlike their work, we calculated these features within the region defined in Fig. 4. The formulae of these features are

$$\text{Mean of magnitude} : M_{\mathrm{ave}} = \frac{1}{L}\sum_{\Omega}|b(f1,f2)| \tag{7}$$

$$\text{Phase entropy} : P_{\mathrm{e}} = \sum_{n} p(\psi_n)\log p(\psi_n) \tag{8}$$

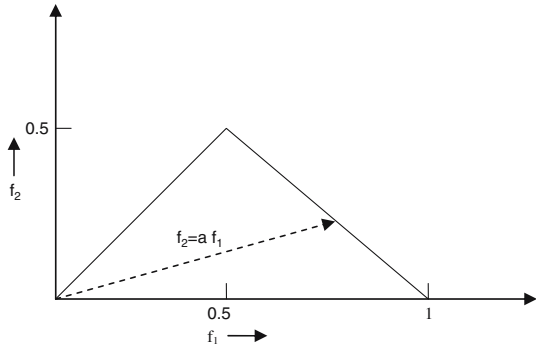

Fig. 4 Non-redundant region of computation of the bispectrum for real signals. Features are calculated by integrating the bispectrum along the *dashed line* with slope ={a. Frequencies are shown normalized by the Nyquist frequency

where

Ω	$\{(f_1, f_2)\mid f_1, f_2$ in the region in Fig. 4$\}$
ψ_n	$\{\phi\mid -\pi+2\pi n/N\leqslant\phi<-\pi+2\pi(n+1)/N,$ $n=0,1,\ldots,N-1$
$p(\psi_n)$	$\frac{1}{L}\sum\Omega 1(\phi(b(f1,f2))\in\psi_n),$ $1(.)=$ indicator function
L	the number of point within the region in Fig. 4
ϕ	refers to the phase angle of the bispectrum.

The formulae for these bispectral entropies are given as

Normalized bispectral entropy(BE1) :

$$\mathrm{P}_1=-\sum_n p_n\log p_n \tag{9}$$

where

$$p_n=\frac{|B(f_1,f_2)|}{\sum_\Omega|B(f_1,f_2)|},$$

Ω, the region as in Fig. 1.

Normalized bispectral squared entropy(BE2) :

$$\mathrm{P}_2=-\sum_n p_n\log p_n \tag{10}$$

where

$$p_n=\frac{|B(f_1,f_2)|^2}{\sum_\Omega|B(f_1,f_2)|^2},$$

Ω the region as in Fig. 4.

Bispectrum and bicoherence plots, mean amplitude of bispectrum, bispectral entropies, invariant features can be used to find different cardiac abnormalities.

2.2.3 Short time fourier transform (STFT)

In order to locate a particular event along the time scale, a finite length window is used at that point. This window may, then be moved along the signal in time producing a succession of estimates of the spectral components of the signal. This works well for signals composed of stationary components and for slowly varying signals. However, for the signal containing, both slowly varying components and rapidly changing transient events, short time fourier transform (STFT) fails. If we use a window of infinite length, we get the FT, which gives perfect frequency resolution, but no time information. Furthermore, in order to obtain the stationarity, we have to have a short enough window, in which the signal is stationary. The narrower we make the window, the better the time resolution, and better the assumption of stationarity, but poorer the frequency resolution.

Wavelet transform [101] overcomes this problem. It uses small windows at the high frequency and longer windows at low frequency. The wavelet can be classified into two types: (1) Discrete wavelet transform (DWT) and (2) CWT.

2.2.4 Continuous time wavelet transform analysis

A *'wavelet'* implies a small wave of finite duration and finite energy, which is correlated with the signal to obtain the wavelet coefficients [130]. The reference wavelet is known as the *mother wavelet*, and the coefficients are evaluated for the entire range of dilation and translation factors [101]. Initially, the mother *wavelet* is shifted (translated) continually along the time scale for evaluating the set of coefficients at all instants of time. In the next phase, the wavelet is dilated for a different width—also normalized to contain the same amount of energy as the mother wavelet—and the process is repeated for the entire signal. The wavelet coefficients are real numbers usually shown by the intensity of a chosen color, against a two-dimensional plane with y-axis representing the dilation (scaling factor) of the wavelet, and the x-axis, its translation (shift along the time axis). Thus, the wavelet transform plot (*scalogram*) can be seen as a color pattern against a two-dimensional plane. In the CWT, the wavelet coefficients are evaluated for infinitesimally small shifts of translation as well as scale factors. That is, the color intensity distribution in the *scalogram* pattern contains information about the location of the 'event' occurring in the time domain [26, 50, 131]. Thus, the color patterns in the scalogram can be useful in highlighting the abnormalities and is specific to different types of diseases.

For a given wavelet $\psi_{a,b}(t)$, the coefficients are evaluated using the equation given below:

$$W(a,b)\equiv\int_{-\infty}^{\infty} f(t)\frac{1}{\sqrt{|a|}}\psi^*\left(\frac{t-b}{a}\right)\mathrm{d}t \tag{11}$$

where

$$\psi^*\left(\frac{t-b}{a}\right)=\psi^*_{a,b}(t);\ a\rightarrow\text{scale factor};$$
$$b\rightarrow\text{translation factor}$$

The *scalogram* patterns thus obtained also depend on the wavelet chosen for analysis. Bio-signals usually exhibit self-similarity patterns in their distribution, and

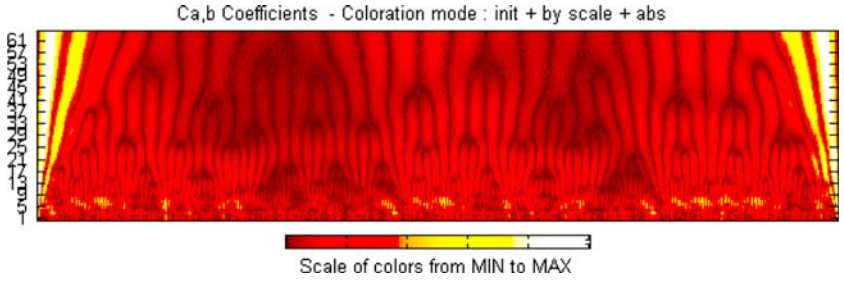

Fig. 5 CWT plot of heart rate signal shown in Fig. 1

a wavelet which is akin to its fractal shape would yield the best results in terms of clarity and distinction of patterns. Figure 5 shows the CWT of the normal HR (shown in Fig. 1) signal using the Morlet mother wavelet [18, 85, 118].

2.3 Nonlinear methods of analysis

Recent developments in the theory of nonlinear dynamics have paved the way for analyzing signals generated from nonlinear living systems [7, 136]. It is now generally recognized that these nonlinear techniques are able to describe the processes generated by biological systems in a more effective way. The technique has been extended here to study of various cardiac arrhythmias. The parameters like correlation dimension (CD), largest Lyapunov exponent (LLE), SD1/SD2 of Poincare plot, ApEn, Hurst exponent, fractal dimension, α slope of DFA and recurrence plots.

2.3.1 Correlation dimension analysis

Recent developments in the theory of nonlinear dynamics have paved the way for analyzing signals generated from nonlinear living systems. It is now generally recognized that these nonlinear techniques are able to describe the processes generated by biological systems in a more effective way. The nonlinear dynamical techniques are based on the concept of chaos and it has been applied to many areas including the areas of medicine and biology. The theory of chaos has been used to detect some cardiac arrhythmias such as VF [60]. Efforts have been made in determining nonlinear parameters like CD for pathological signals and it has been shown that they are useful indicators of pathologies. Methods based on chaos theory have been applied in tracking HRV signals and predicting the onset events such as ventricular tachycardia for detecting congestive heart failure situations [27]. A novel method based on phase space technique to distinguish normal and abnormal cases has been proposed for cardiovascular signals [81]. The technique has been extended here to identify the abnormalities of different types.

In the phase space plot shown X-axis represents the heart-rate $X[n]$ and the Y-axis represents the heart-rate after a delay $X[n + \text{delay}]$. The choice of an appropriate delay is calculated using the minimal mutual information technique [42, 43]. Figure 6 shows the phase space plot of the normal subject (shown in Fig. 1). The spread of the phase space plot is different for various cardiac abnormalities [3, 4].

Correlation dimension is one of the most widely used measures of fractal dimension. Here, the algorithm proposed by Grassberger et al. [48] is adapted. The idea is to construct a function $C(r)$, i.e., the probability that two arbitrary points on the orbit are closer together than r. This is done by calculating the separation between every pair of N data points and sorting them into bins of width dr proportionate to r. A CD can be calculated using the distances between each pair of points in the set of N number of points, $s(i,j) = | X_i - X_j |$

A correlation function, $C(r)$, is then calculated using, $C(r) = \frac{1}{N^2} \times (\text{Number of pairs of } (i,j) \text{ with } s(i,j) < r)$. $C(r)$ has been found to follow a power law similar to the one seen in the capacity dimension: $C(r) = kr^D$. Therefore, we can find CD with estimation techniques derived from the formula:

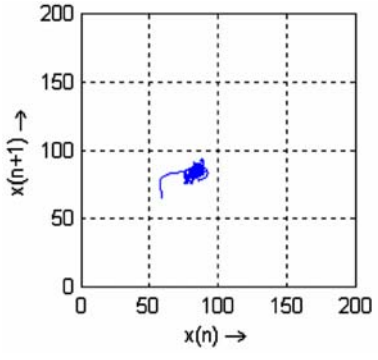

Fig. 6 Phase space plot of normal heart rate signal shown in Fig. 1

$$\mathrm{CD} = \lim_{r \to 0} \frac{\log(C(r))}{\log(r)} \tag{12}$$

The CD value will be high for the chaotic data and it decreases as the variation of RR signal becomes less or rhythmic. The CD is more for NSR and it decreases for different cardiac diseases [3, 4]. The embedding dimension of 10 and time delay of 1 is chosen for the HR signals. The CD is 3.61 for the HR signal shown in Fig. 1.

2.3.2 Detrended fluctuation analysis

The DFA is used to quantify the fractal scaling properties of short interval RR interval signals. This technique is a modification of root-mean-square analysis of random walks applied to nonstationary signals [55]. The root-mean-square fluctuation of an integrated and detrended time series is measured at different observation windows and plotted against the size of the observation window on a log–log scale.

First, the RR time series (of total length K) is integrated using the equation:

$$y(k) = \sum_{i=1}^{k} \left[\mathrm{RR}(i) - \mathrm{RR}_{\mathrm{avg}}\right] \tag{13}$$

where $y(k)$ is the kth value of the integrated series, $\mathrm{RR}(i)$ is the ith inter beat interval, and the $\mathrm{RR}_{\mathrm{avg}}$ is the average inter beat interval over the entire series.

Then, the integrated time series is divided into windows of equal length, n. In each window of length n, a least-squares line is fitted to the RR interval data (representing the trend in that window). The y coordinate of the straight line segments are denoted by $y_n(k)$. Next, we detrend the integrated time series, $y_n(k)$, in each window. The root-mean-square fluctuation of this integrated and detrended series is calculated using the equation:

$$F(n) = \sqrt{1/N \sum_{k=1}^{N} [y(k) - y_n(k)]^2} \tag{14}$$

This computation is repeated over all time scales (window sizes) to obtain the relationship between $F(n)$ and the window size n (i.e., the number of beats in a window that is the size of the window of observation). Typically, $F(n)$ will increase with window size. The fluctuation in small windows are related to the fluctuations can be characterized by a scaling exponent (self-similarity factor), $\propto$, representing the slope of the line relating log $F(n)$ to log (n). In this method, a fractal-like signal results in a scaling exponent value of 1 ($\propto = 1$). White Gaussian noise (totally random signal) results in a value of 0.5, and a Brownian noise signal with spectrum rapidly decreasing power in the higher frequencies results in an exponent value of 1.5 [54, 55]. The $\propto$ can be viewed as an indicator of the ''roughness'' of the original time series: the larger the value of the $\propto$ the smoother the time series.

The fractal scaling ($\propto$) for the normal subjects (healthy young) it is closer to 1, and this value falls in different ranges for various types of cardiac abnormalities. This slope very low for low very highly varying signals like PVC, LBBB, AF and VF. But for rhythmically varying signals like SSS, CHB and Ischemic/dilated cardiomyopathy this value is slightly higher (comparable to 1) [3, 4]. The $\propto$ slope is 0.7707 for the HR signal shown in Fig. 1.

2.3.3 Largest Lyapunov exponent

Lyapunov exponent (λ) is a quantitative measure of the sensitive dependence on the initial conditions. It defines the average rate of divergence of two neighboring trajectories. An exponential divergence of initially nearby trajectories in phase space coupled with folding of trajectories, ensure that the solutions will remain finite, is the general mechanism for generating deterministic randomness and unpredictability. Therefore, the existence of a positive λ for almost all initial conditions in a bounded dynamical system is widely used. To discriminate between chaotic dynamics and periodic signals Lyapunov exponent (λ) are often used. It is a measure of the rate at which the trajectories separate one from other. The trajectories of chaotic signals in phase space follow typical patterns. Closely spaced trajectories converge and diverge exponentially, relative to each other. For dynamical systems, sensitivity to initial conditions is quantified by the Lyapunov exponent (λ). They characterize the average rate of divergence of these neighboring trajectories. A negative exponent implies that the orbits approach a common fixed point. A zero exponent means the orbits maintain their relative positions; they are on a stable attractor. Finally, a positive exponent implies the orbits are on a chaotic attractor.

The algorithm proposed by Wolf et al. [142] is used to determine the LLE. For two nearby points in a space $\mathbf{x}_0$ and $\mathbf{x}_0 + \Delta\mathbf{x}$, that are function of time and each of which will generate an orbit of its own in the state, the separation between the two orbits $\Delta\mathbf{x}$ will also be a function of time. This separation is also a

function of the location of the initial value and has the form $\Delta\mathbf{x}(\mathbf{x}_0, t)$. For chaotic data set, the mean exponential rate of divergence of two initially close orbits is characterized by,

$$\lambda = \lim_{t\to\infty} \frac{1}{t} \ln \frac{|\Delta\mathbf{x}(\mathbf{x}_0, t)|}{|\Delta\mathbf{x}|}. \tag{15}$$

The maximum positive λ is chosen as λ_1.

Largest Lyapunov exponent's quantify sensitivity of the system to initial conditions and gives a measure of predictability. This value decreases for slowly varying signals like CHB and Ischemic/dilated cardiomyopathy and will be higher for the other cases as the variation of RR is more [3, 4]. The LLE is 0.505 for the HR signal shown in Fig. 1.

2.3.4 Approximate entropy

Pincus [93] proposed ApEn as a solution to these problems and successfully applied it to relatively short and noisy data. ApEn is scale invariant and model independent and discriminates time series for which clear future recognition is difficult. ApEn detects the changes in underlying episodic behavior not reflected in peak occurrences or amplitudes [95]. ApEn assigns a nonnegative number to a time series, with larger values corresponding to more complexity or irregularity in the data [93]. For N data points $x(1)$, $x(2)$,..., $x(N)$, with an embedding space of $\Re^m$, the ApEn measure is given by

$$\begin{aligned}\mathrm{ApEn}(m, r, N) = &\frac{1}{N-m+1}\sum_{i=1}^{N-m+1} \log C_i^m(r) \\ &- \frac{1}{N-m}\sum_{i=1}^{N-m} \log C_i^{m+1}(r)\end{aligned} \tag{16}$$

where $C_i^m(r) = \frac{1}{N-m+1}\sum_{lj=1}^{N-m+1} \Theta\left(r - \left\|\mathbf{x}_i - \mathbf{x}_j\right\|\right)$ is the correlation integral. The values of m and r may be chosen based on the results of previous studies by Pincus [94] indicating good statistical validity for ApEn.

The importance of ApEn lies in the fact that it is measure of the disorder in the HR signal. It is a measure, quantifying the regularity and complexity of time series. It has higher value in the case of normal and SSS subjects and it falls as the RR variation decreases. Hence, the ApEn will have smaller value for cardiac abnormal cases, indicating smaller variability in the beat to beat. But, for SSS this RR variation will be higher than the normal subjects [3, 4]. The ApEn is 2.2705 for the HR signal shown in Fig. 1.

2.3.5 Fractal dimension

The term "fractal" was first introduced by Mandelbrot [77]. A fractal is a set of points that when looked at smaller scales, resembles the whole set. The concept of fractal dimenstion (FD) that refers to a noninteger or fractional dimension originates from fractal geometry. The FD emerges to provide a measure of how much space an object occupies between Euclidean dimensions. The FD of a waveform represent a powerful tool for transient detection. This feature has been used in the analysis of ECG and EEG to identify and distinguish specific states of physiologic function. Many algorithms are available to determine the FD of the waveform. In this work, algorithms proposed by Higuchi and Katz are implemented for analysis of ECG and EEG signals.

Higuchi's algorithm Consider $x(1), x(2),..., x(N)$ the time sequence to be analyzed. Construct k new time series x_m^k as $x_m^k = \{x(m), x(m+k), x(m+2k), \ldots..., x(m+[N-mk]k),\}$ for $m = 1, 2, ..., k$, where m indicates the initial time value, and k indicates the discrete time interval between points, and $\lfloor a \rfloor$ means the integer part of a. For each of the k time series or curves $x^k{}_m$, the length $L_m(k)$ is computed by,

$$L_m(k) = \frac{\sum_{i=1}^{\lfloor a \rfloor} |x(m+ik) - x(m+(i-1)k)|(N-1)}{\lfloor a \rfloor k} \tag{17}$$

where N is the total length of the data sequence x, $(N-1)/\lfloor a \rfloor k$ is a normalization factor and $a = \frac{N-m}{k}$. An average length is computed as the mean of the k lengths $L_m(k)$ for $m = 1, 2,..., k$. This procedure is repeated for each k ranging from 1 to $k_{\max}$, obtaining an average length for each k. In the curve of $\ln(L_m(k))$ versus $\ln(1/k)$, the slope of the least-squares linear best fit is the estimate of the FD (D^{Higuchi}) [53]. The D^{Higushi} is 1.3604 for the HR signal shown in Fig. 1.

Katz algorithm Using Katz's method [62] the FD of a curve can be defined as,

$$D^{\mathrm{Katz}} = \frac{\log_{10}(L)}{\log_{10}(d)} \tag{18}$$

where L is the total length of the curve or sum of distances between successive points, and d is the diameter estimated as the distance between the first point of the sequence and the point of the sequence that provides the farthest distance. Mathematically, d can be expressed as $d = \max(\|x(1), x(i)\|)$.

Considering the distance between each point of the sequence and the first, point *i* is the one that maximizes the distance with respect to the first point. The FD compares the actual number of units that compose a curve with the minimum number of units required to reproduce a pattern of the same spatial extent. FDs computed in this fashion depend upon the measurement units used. If the units are different, then so are the FDs. Katz's approach solves this problem by creating a general unit or yardstick: the average step or average distance between successive points, *a*. Normalizing the distances D^{katz} is then given by,

$$D^{\text{Katz}} = \frac{\log_{10}(L/a)}{\log_{10}(d/a)} \tag{19}$$

The D^{Katz} is 1.5801 for the HR signal shown in Fig. 1.

2.3.6 Hurst exponant (H)

The Hurst exponent is a measure that has been widely used to evaluate the self-similarity and correlation properties of fractional Brownian noise, the time series produced by a fractional (fractal) Gaussian process. Hurst exponent is used to evaluate the presence or absence of long-range dependence and its degree in a time series. However, local trends (nonstationarities) is often present in physiological data and may compromise the ability of some methods to measure self-similarity. Hurst exponent is the measure of the smoothness of a fractal time series based on the asymptotic behavior of the rescaled range of the process. The Hurst exponent *H* is defined as,

$$H = \log(R/S)/\log(T) \tag{20}$$

where *T* is the duration of the sample of data and *R/S* the corresponding value of rescaled range. The above expression is obtained from the Hurst's generalized equation of time series that is also valid for Brownian motion. If $H = 0.5$, the behavior of the time series is similar to a random walk. If $H < 0.5$, the time-series cover less ''distance'' than a random walk. But if $H > 0.5$, the time-series covers more ''distance'' than a random walk. *H* is related to the dimension CD given by,

$$H = E + 1 - \text{CD}. \tag{21}$$

Here, *E* is the Euclidean dimension.

For normal subjects, the FD is high due to the variation being chaotic. And for CHB and Ischemic/dilated cardiomyopathy, this FD decreases because the RR variation is low. And for AF and SSS, this FD value falls further, because the RR variation becomes erratic or periodic respectively [3, 4]. The *H* is 0.611 for the HR signal shown in Fig. 1.

2.3.7 Sample entropy (SampEn)

Richman and Randall [103] have developed and characterized SampEn, a new family of statistics measuring complexity and regularity of clinical and experimental time-series data and compared it with ApEn, a similar family. SampEn statistics provide an improved evaluation of time-series regularity and is a useful tool in studies of the dynamics of human cardiovascular physiology as compared to the ApEn.

The SampEn is very similar to the ApEn, but there is a small computational difference [102]. In ApEn, the comparison between the template vector and the rest of the vectors also includes comparison with itself. This guarantees that probabilities $C^{m}{}_{i}\,(r)$ are never zero. Thus it is always possible to take a logarithm of probabilities. Because template comparisons with itself lower ApEn values, the signals are interpreted to be more regular than they actually are.

With SampEn, the vector comparison with itself is removed

$$C_i^{'m}(r) = \{\text{the number of } j, j \neq i, j \leqslant N-m+1, \text{ such that } d[u(i),u(j)] \leqslant r\}/(N-m+1) \tag{22}$$

Now we can determine

$$\phi^{'m}(r) = (N-m+1)^{-1} \sum_{i=1}^{N-m+1} C_i^{'m}(r) \tag{23}$$

and finally

$$\text{SampEn}(m,r,N) = -\ln\left[\phi^{'m}(r) \Big/ \phi^{'m+1}(r)\right] \tag{24}$$

SampEn measures complexity of the signal in the same manner as ApEn. However, the dependence on the parameters *N* and *r* is different. SampEn decreases monotonically when *r* increases. In theory, SampEn does not depend on *N*. In analyzing time series including <200 data points, however, the confidence interval of the results is unacceptably large. When *r* and *N* are large, SampEn and ApEn give the same results. The SampEn is 1.36 for the heart rate signal shown in Fig. 1.

2.3.8 *Recurrence plots*

In time-series analysis, the dynamic properties of the data under consideration are relevant and valid only, if the data is stationary. Recurrence plots are used to reveal nonstationarity of the series. These plots were first proposed by Eckmann et al. [33] as graphical tool for the diagnosis of drift and hidden periodicities in the time evolution, which are unnoticeable otherwise. A brief description on the construction of recurrence plots is described below.

Let $\mathbf{x}_i$ be the ith point on the orbit in an m-dimensional space. The recurrence plot is an array of dots in an $N \times N$ square, where a dot is placed at (i,j) whenever $\mathbf{x}_j$ is sufficiently close to $\mathbf{x}_i$. To obtain the recurrence plot, m-dimensional orbit of $\mathbf{x}_i$ is constructed. A radius r such that the ball of radius r centered at $\mathbf{x}_i$ in $\Re^m$ contains a reasonable number of other points $\mathbf{x}_j$ of the orbit. Finally, a dot is plotted for each point (i,j) for which $\mathbf{x}_j$ is in the ball of radius r centered at $\mathbf{x}_i$. The plot thus obtained is the recurrence plot. The plots will be symmetric along the diagonal $i = j$, because if $\mathbf{x}_i$ is close to $\mathbf{x}_j$, then $\mathbf{x}_j$ is close to $\mathbf{x}_i$. The recurrence plot of normal HR (shown in Fig. 1) is given in Fig. 7. For *normal* cases, the RP has diagonal line and less squares indicating more variation indicating high variation in the HR. Abnormalities like *CHB* and in Ischemic/dilated cardiomyopathy cases, show more squares in the plot indicating the inherent periodicity and the lower HR variation [25].

3 Requirements for nonlinear analysis

Specifics of the biological systems require modifications of standard nonlinear dynamics algorithms. The main problems of the nonlinear analysis, when applying it to biological signals can be summarized as follows: (a) high level of random noise in the biological data. The applied nonlinear dynamics methods should be robust to the noise influence; (b) short experimental data sets due to the low frequencies of the biological signals. Short realizations cause large error bars in the estimation of the chaos parameters; (c) nonstationarity of the biological systems, i.e., ECG, EEG have different modulations influenced by a various external factors with different characteristic times; (d) spatially extended character of the system.

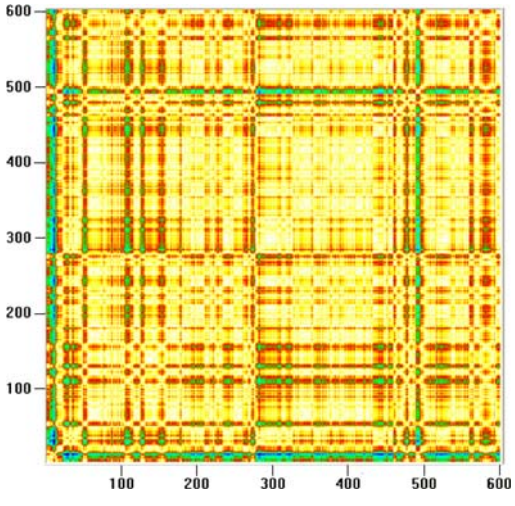

Fig. 7 Recurrence plot of normal heart rate (shown in Fig. 1)

3.1 Surrogate data

It is necessary to check the data for the nonlinearity. One of the tests for nonlinearity is the surrogate data test.

The method of using surrogate in nonlinear time-series analysis was introduced by Theiler et al. [121]. Surrogate signal is produced by phase randomizing the original data. It has similar spectral properties as of the given data. The surrogate data sequence has the same mean, the same variance, the same autocorrelation function and therefore the same power spectrum as the original sequence, but phase relations are destroyed. In the case of data shuffling the histograms of the surrogate sequence and the reference sequence are identical. The random phase spectrum is generated by using any of the three methods described below.

1. Random phase: here the complex phase values of the Fourier transformed input signal are chosen randomly.
2. Phase shuffle: here the phase values of the original spectrum are used in random order.
3. Data shuffle: here the phase values of the original spectrum are used in random order and the sorted values of the surrogate sequence are substituted by the corresponding sorted values of the reference sequence additionally.

The measured topological properties of the experimental time series are then compared with that of the measured topological properties of the surrogate data sets. If both the experimental data and the surrogate data yield the same results then the null hypothesis that the experimental data is set of random noise and the underlying process is linear.

4 Discussion

Statistical, geometric, frequency domain, time-frequency and nonlinear parameters have been discussed

in detail in the previous sections. Conventionally, HR fluctuation has been assessed by calculating indices based on statistical operations on RR intervals (means and variance). The most widely used time domain index is the average HR, SDNN and RMSSD. All the time domain measure indices could be affected by artifacts and outliers, and these measures therefore require data from which artifacts and ectopic beats have been carefully eliminated.

Geometrical methods present RR intervals in geometric patterns and triangular index, Poincare plots have been used to derive measures of HR signals. This triangular index had a high correlation with the standard deviation of all RR intervals, but it is highly insensitive to artifacts and ectopic beats, because they are left outside the triangle.

Experience with frequency domain analysis over the past two decades strongly suggests that it represents a unique, noninvasive tool for achieving a more precise assessment of autonomic function in both the experimental and clinical settings. Available studies indicate that the significance of the HF component is far better understood than that of the lower frequency components. Respiratory pattern also can significantly influence HF power. The use of controlled breathing minimizes these problems, improves reproducibility of test findings, and also facilitates quantitative comparisons. The situation with respect to LF power is more complicated because it is modulated by both sympathetic and parasympathetic outflows as well as by other factors, including baroreceptor activity. Therefore, LF analysis per se cannot afford a precise delineation of the state of sympathetic activation. The meaningful determinations of VLF and ULF power may be difficult because decrease in frequency to such low levels are associated with an increasing propensity to violate the rules governing power spectral determinations, violations that diminish reliability despite the most sophisticated preprocessing. It is also noteworthy that the reliability of spectral power determinations diminishes with decreases in the power of the signal and of the signal-to-noise ratio.

The wavelet transform has become a valuable analysis tool due to its ability to elucidate simultaneously both spectral and temporal information within the signal. This overcomes the basic shortcoming of Fourier analysis, which is that the Fourier spectrum contains only globally averaged information, so leading to location specific features in the signal being lost.

There is increasing evidence to suggest that the heart is not a periodic oscillator under normal physiologic conditions [47], and the commonly employed moment statistics of HRV may not be able to detect subtle, but important changes in HR time series. Therefore several new analysis method of HR behavior, motivated by nonlinear dynamics and chaos theory, have been developed to quantify the dynamics of HR fluctuations [47, 93]. ApEn is a measure and parameter that quantifies the regularity or predictability of time-series data. This shows higher values for the normal heart signals and will have smaller values for the cardiac abnormal signals [3, 4].

The DFA technique is a measurement which quantifies the presence or absence of fractal correlation properties and has been validated for time-series data [91]. It was developed to characterize fluctuations on scales of all lengths. The self-similarity occurring over an large range of time scales can be defined for a selected time scale with this method. The fractal scaling ($\propto$) for the normal subjects (healthy young) it is closer to 1, and this value falls in different ranges for various types of cardiac abnormalities. This slope very low for low very highly varying signals like PVC, LBBB, AF andVF. But for rhythmically varying signals like SSS, CHB and Ischemic/Dilated cardiomyopathy this value is slightly higher (comparable to 1) [3, 4]. The Lyapunov exponent is a quantitative measure of separation of the divergence of the trajectories from their initial close positions. The magnitude of this exponent indicates the intensity of the chaotic the system. This value decreases for slowly varying signals like CHB and Ischemic/dilated cardiomyopathy and will be higher for the other cases as the variation of RR is more [3, 4].

When the HR is steady and unchanging, the phase-space plot reduces to a point, but otherwise, the trajectory spreads out to give some patterns on the screen. The pattern that emerges can be interpreted for finer details—such as whether the HR is periodic, chaotic, or random, etc. A CD factor is defined to obtain a quantitative measure of the nature of trajectory of the phase space plot. It has higher values for normal HR signals and this value falls as the beat to beat variation falls [3, 4]. Hurst Exponent is the measure of the smoothness of a fractal time series based on the asymptotic behavior of the rescaled range of the process. The cardiac abnormalities like AF, SSS, VF, PVC, CHB, Ischemic/dilated cardiomyopathy have slightly higher values as compared to the normal HR. This is because of the presence of the inherent rhythm in these HR data. Similarly, FD allows us to measure the degree of complexity by evaluating how fast our measurements increase or decrease as our scale becomes larger or smaller. These values will be higher for the normal subjects and small for the abnormal subjects due to reduced or rhythmic variation.

Slowly varying HR diseases like, CHB, Ischemic/dilated cardiomyopathy have more number of squares in the RP. This is due to the inherent periodicity of the time series. The RP show more patches of colors in cardiac diseases, where the HR signal is highly varying signals [25]. Censi et al. [23] performed a quantitative study of coupling patterns between respiration and spontaneous rhythms of HR and BP variability signals by using the recurrence quantification analysis (RQA). They applied RQA to both simulated and experimental data obtained in control breathing at three different frequencies (0.25, 0.20, and 0.13 Hz) from ten normal subjects. RP concept was used to detect the life threatening arrhythmias like ventricular tachycardias [78].

Jamsek et al. [56] used bispectral analysis to study the coupling between cardiac and respiratory activity. Witte et al. [141] too studied the coupling between cardiac and respiratory activity but this research was on neonatal subjects. Pinhas et al. [96] have used the bispectrum to analyze the coupling between BP and HRV in heart transplant patients.

5 Conclusion

Heart rate variability analysis has become an important tool in cardiology, because its measurements are noninvasive and easy to perform, have relatively good reproducibility and provide prognostic information on patients with heart disease. HRV has proved to be a valuable tool to investigate the sympathetic and parasympathetic function of the ANS, especially in diabetic and postinfarction patients. Spectral analysis of HR has clarified the nature of diabetic autonomic neuropathy and of other neurologic disorders that encounter the ANS. Nonlinear parameters can be used to analyze the health of the subjects. In the future, individual therapy adjustments to aim at the most favorable sympathetic-parasympathetic balance in postinfarction patients might be possible with the help of HRV analysis.

References

1. Acharya UR, Min LC, Joseph P (2002) HRV analysis using correlation dimension and DFA. Innov Tech Biol Med (ITBM-RBM) 23:333–339
2. Acharya UR, Bhat PS, Iyengar SS, Rao A, Dua S (2003) Classification of heart rate using artificial neural network and fuzzy equivalence relation. Pattern Recogn 36:61–68
3. Acharya UR, Kannathal N, Krishnan SM (2004) Comprehensive analysis of cardiac health using heart rate signals. Physiol Meas J 25:1130–1151
4. Acharya UR, Kannathal N, Seng OW, Ping LY, Chua T (2004) Heart rate analysis in normal subjects of various age groups. Biomed Online J USA 3(24)
5. Akaike H (1969) Fitting autoregressive models for prediction. Ann Inst Stat Math 21:243–247
6. Akaike H (1974) A new look at statistical model identification. IEEE Trans Autom Control 19:716–723
7. Akay M (2001) Nonlinear biomedical signal processing dynamic analysis and modeling, vol II. IEEE Press, New York
8. Akselrod S, Gordon D, Ubel FA, Shannon DC, Barger MA, Cohen RJ (1981) Power spectrum analysis of heart rate fluctuation. Science 213:220–222
9. Akselrod S, Gordon D, Madwed J, Snidman N, Shannon D, Cohen R (1985) Hemodynamic regulation: investigation by spectral analysis. Am J Physiol 249:H867–H875
10. Axelrod S, Lishner M, Oz O, Bernheim J, Ravid M (1987) Spectral analysis of fluctuations in heart rate: an objective evaluation of autonomic nervous control in chronic renal failure. Nephron 45:202–206
11. Barutcu I, Esen AM, Kaya D, Turkmen M, Karakaya O, Melek M, Esen OB, Basaran Y (2005) Cigarette smoking and heart rate variability: dynamic influence of parasympathetic and sympathetic maneuvers. Ann Noninvas Electrocardiol 10(3):324–329
12. Bekheit S, Tangella M, el-Sakr A, Rasheed Q, Craelius W, el-Sherif N (1990) Use of heart rate spectral analysis to study the effects of calcium channel blockers on sympathetic activity after myocardial infarction. Am Heart J 119:79–85
13. Berger RD,Akselrod S,Gordon D,Cohen RJ (1986) An efficient algorithm for spectral analysis of heart rate variability. IEEE Trans Biomed Eng 33:900–904
14. de Boer RW, Karemaker JM, Strackee J (1985) Relationships between short-term blood-pressure fluctuations and heart-rate variability in resting subjects. I: a spectral analysis approach. Med Biol Eng Comput 23(4):352–358
15. de Boer RW, Karemaker JM, Strackee J (1985) Relationships between short-term blood-pressure fluctuations and heart-rate variability in resting subjects. II: a simple model. Med Biol Eng Comput 23(4):359–64
16. de Boer RW, Karemaker JM, Strackee J (1985) Spectrum of a series of point events, generated by the integral pulse frequency modulation model. Med Biol Eng Comput 23(2):138–142
17. Bonnemeier H, Wiegand UKH, Brandes A, Kluge N, Katus HA, Richardt G, Potratz J (2003) Circadian profile of cardiac autonomic nervous modulation in healthy subjects: Differing Effects of aging and Gender on heart rate variability. J Cardiovasc Electrophysiol 14:8791–799
18. Bracic M, Stefanovska A (1998) Wavelet-based analysis of human blood-flow dynamics. Bull Math Biol 60:919–935
19. Broadman A, Schlindwein FS, Rocha AP, Leite A (2002) A study on the optimum order of autoregressive models for heart rate variability. Physiol Meas 23:324–36
20. Bušek P, Vaòková J, Opavský J, Salinger J, Nevšímalová S (2005) Spectral analysis of heart rate variability in sleep. Physiol Res 54:369–376
21. Carney RM, Blumenthal JA, Stein PK, Watkins L, Catellier D, Berkman LF, Czajkowski SM, O'Connor C, Stone PH, Freedland KE (2001) Depression, heart rate variability, and acute myocardial infarction. Circulation 104:2024
22. Carney RM, Blumenthal JA, Freedland KE, Stein PK, Howells WB, Berkman LF, Watkins LL, Czajkowski SM, Hayano J, Domitrovich PP, Jaffe AS (2005) Low heart rate

variability and the effect of depression on post—myocardial infarction mortality. Arch Intern Med 165:1486–1491
23. Censi F, Calcagnini G, Cerutti S (2002) Coupling patterns between spontaneous rhythms and respiration in cardiovascular variability signals. Comput Meth Programs Biomed 68(1):37–47
24. Chandran V, Elgar S (1993) Pattern recognition using invariants defined from higher order spectra—one-dimensional inputs. IEEE Trans Signal Process 41:1
25. Chua KC, Chandran V, Acharya UR, Min LC (2006) Computer-based analysis of cardiac state using entropies, recurrence plots and Poincare geometry. J Med Eng Technol UK (in press)
26. Chui CK (1992) Wavelet analysis and its applications. Acadamic, Boston, MA
27. Cohen ME, Hudson DL, Deedwania PC (1996) Applying continuous chaotic modeling to cardiac signal analysis. IEEE Eng Med Biol 15:97–102
28. Coumel P, Hermida JS, Wennerblom B, Leenhardt A, Maison-Blanche P, Cauchemez B (1991) Heart rate variability in left ventricular hypertrophy and heart failure, and the effects of beta-blockade. Eur Heart J 12:412–422
29. Cysarz D, Bettermann H, van Leeuwen P (2000) Entropies of short binary sequences in heart period dynamics. Am J Physiol Heart Circ Physiol 278:H2163–H2172
30. Davy KP, Desouza CA, Jones PP, Seals DR (1998) Elevated heart rate variability in physically active young and older adult women. Clin Sci 94:579–584
31. Drinnan MJ, Allen J, Langley P, Murray A (2000) Detection of sleep apnoea from frequency analysis of heart rate variability. Comput Cardiol 27:259–62
32. Duru F, Candinas R, Dziekan G, Goebbels U, Myers J, Dubach P, Chur K (2000) Effect of exercise training on heart rate variability in patients with new-onset left ventricular dysfunction after myocardial infarction. Am Heart J 140(1):157–161
33. Eckmann JP, Kamphorst SO, Ruelle D (1987) Recurrence plots of dynamical systems. Europhys Lett 4:973–977
34. Elsenbrunch S, Harnish MJ, Orr WC (1999) Heart rate variability during waking and sleep in healthy males and females. Sleep 22(8):1067–1071
35. Emese N, Hajnalka O, Bardos G, Molnar P (2000) Gender-related heart rate differences in human neonates. Pediatr Res 47(6):778–780
36. Eryonucu B, Uzun K, Güler N, Bilge M (2001) Comparison of the acute effects of salbutamol and terbutaline on heart rate variability in adult asthmatic patients. Eur Respir J 17:863–867
37. Ewing DJ, Winney R (1975) Autonomic function in patients with chronic renal failure on intermittent haemodialysis. Nephron 15(6):424–429
38. Farrell TG, Bashir Y, Cripps T, Malik M, Poloniecki J, Bennett ED, Ward DE, Camm AJ (1991) Risk stratification for arrhythmic events in postinfarction patients based on heart rate variability, ambulatory electrocardiographic variables and the signal-averaged electrocardiogram. J Am Coll Cardiol 18:687–697
39. Fell J, Mann K, Roschke J, Gopinathan MS (2000) Nonlinear analysis of continuous ECG during sleep I. Reconstruction. Biol Cybernat 82:477–483
40. Finley JP, Nungent ST, Hellenbrand W (1987) Heart rate variability in children, spectral analysis of developmental changes between 5 and 25 years. Can J Physiol Pharmacol 65:2048–2052
41. Forsstrom J, Forsstrom J, Heinonen E, Valimaki I, Antila K (1986) Effects of haemodialysis on heart rate variability in chronic renal failure. Scand J Clin Lab Invest 46:665–670
42. Fraser AM (1989) Information and entropy in strange attractors. IEEE Trans Inform Theory 35:245–262
43. Fraser AM, Swinney HL (1986) Independent coordinates for strange attractors from mutual information. Phys Rev A 33:1134–1140
44. Gamero LG, Vila J, Palacios F (2002) Wavelet transform analysis of heart rate variability during myocardial ischaemia. Med Biol Eng Comput 40:72–78
45. Gates GJ, Mateika SE, Mateika JH (2005) Heart rate variability in non-apneic snorers and controls before and after continuous positive airway pressure. BMC Pulm Med 5:9
46. Ge D, Srinivasan N, Krishnan SM (2002) Cardiac arrhythmia classification using autoregressive modeling. BioMed Eng Online 1(1):5
47. Goldberger AL, West BJ (1987) Application of nonlinear dynamics to clinical cardiology. Ann NY Acad Sci 504:195–213
48. Grassberger P, Procassia I (1983) Measuring the strangeness of strange attractors. Physica D 9:189–208
49. Grossman P, Karemaker J, Wieling W (1991) Prediction of tonic parasympathetic cardiac control using respiratory sinus arrhythmia: the need for respiratory control. Psychophysiology 28:201–216
50. Grossmann A, Kronland-Martinet R, Morlet J (1989/1990) Reading and understanding continuous wavelet transforms. In: Combes JM, Grossmann A, Tchamitchian Ph (eds) Wavelets: time-frequency methods and phase space. Springer, Berlin Heidelberg New York, pp 2–20
51. Guzzetti S, Piccaluga E, Casati R, Cerutti S, Lombardi F, Pagani M et al (1988) Sympathetic predominance in essential hypertension: a study employing spectral analysis of heart rate variability. J Hypertens 6:711–717
52. Hayano J, Yamada M, Sakakibara Y et al (1990) short, longterm effects of cigarette smoking on heart rate variability. Am J Cardiol 65:84–88
53. Higuchi T (1988) Aproach to an irregular time series on the basis of the fractal theory. Physica D 31:277–283
54. Ho KK, Moody GB, Peng CK, Meitus JE, Larson MG, Levy D, Goldberger AL (1997) Predicting survival in heart failure case and control subjects by use of fully automated methods for deriving nonlinear and conventional indices of heart rate dynamics. Circulation 96:842–848
55. Huikuri HV, Makikallio TH, Peng CK, Goldberger AL, Hintze U, Moller M (2000) Fractal correlation properties of R–R interval dynamics and mortality in patients with depressed left ventricular function after an acute myocardial infarction. Circulation 101:47–53
56. Jamsek J, Stefanovska A, McClintock PVE (2004) Nonlinear cardio-respiratory interactions revealed by time-phase bispectral analysis. Phys Med Biol 49:4407–4425
57. Kamath MV, Fallen EL (1993) Power spectral analysis of heart rate variability: a noninvasive signature of cardiac autonomic function. Crit Rev Biomed Eng 21(3):245–311
58. Kamath MV, Fallen EL (1995) Correction of the heart rate vaiability signal for ectopics and missing beats. In: Malik M, Camm AJ (eds) Heart rate variability. Futura, Armonk, pp 75–85
59. Kamen PW, Krum H, Tonkin AM (1996) Poincare plot of heart rate variability allows quantitative display of parasympathetic nervous activity. Clin Sci 91:201–208
60. Kaplan DK, Cohen JR (1991) Searching for chaos in fibrillation. Ann NY Acad Sci 367–374

61. Katona PG, Jih F (1975) Respiratory sinus arrhythmia: noninvasive measure of parasympathetic cardiac control. J Appl Physiol 39:801–805
62. Katz MJ (1988) Fractals and analysis of waveforms. Comput Biol Med 18:145–156
63. Kleiger RE, Bigger JT, Bosner MS, Chung MK, Cook JR, Rolnitzky LM et al (1991) Stability over time of variables measuring heart rate variability in normal subjects. Am J Cardiol 68:626–630
64. Kobayashi M,Musha T (1982) 1/f fluctuation of heart beat period. IEEE Trans Biomed Eng 29:456–457
65. Kovatchev BP, Farhy LS, Cao H, Griffin MP, Lake DE, Moorman JR (2003) Sample asymmetry analysis of heart rate characteristics with application to neonatal sepsis and systemic inflammatory response syndrome. Pediatr Res 54:892–898
66. Laude D, Elghozi JL, Girald A, Bellard E, Bouhaddi M, Castiglioni P et al (2004) Comparison of various techniques used to estimate spontaneous baroreflex sensitivity (the EUROVAR study). Am J Physiol Regul Integr Comp Physiol 286:R226–R231
67. Leipzig TJ, Lowensohn RI (1986) Heart rate variability in neurosurgical patients. Neurosurgery 19:356–362
68. Lerma C, Minzoni A, Infante O, José MV (2004) A mathematical analysis for the cardiovascular control adaptations in chronic renal failure. Artif Organs 28(4):398–409
69. Levy MN,Schwartz PJ (eds) (1994) Vagal control of the heart: experimental basis and clinical implications. Future, Armonk
70. Lipsitz LA, Mietus J, Moody GB, Goldberger AL (1990) Spectral characteristics of heart rate variability before and during postural tilt: relations to aging and risk of syncope. Circulation 81:1803–1810
71. Lowensohn RI, Weiss M, Hon EH (1977) Heart-rate variability in brain-damaged adults. Lancet 1:626–628
72. Luchini D, Bertocchi F, Maliani A et al. (1996) A controlled study of the autonomic changes produced by habitual cigarette smoking in healthy subjects. Cardiovasc Res 31:633–639
73. Mager DE, Merritt MM, Kasturi J, Witkin LR, Urdiqui-Macdonald M, Sollers JJ III, Evans MK, Zonderman AB, Abernethy DR, Thayer JF (2004) Kullback–Leibler clustering of continuous wavelet transform measures of heart rate variability. Biomed Sci Instrum 40:337–342
74. Malik M, Farrell T, Cripps TR, Camm AJ (1989) Heart rate variability in relation to prognosis after myocardial infarction: selection of optimal processing techniques. Eur Heart J 10:1060–1074
75. Malliani A, Pagani M, Lombardi F, Cerutti S (1991) Cardiovascular neural regulation explored in the frequency domain. Circulation 84:482–92
76. Malpas SC, Whiteside EA, Maling TJ (1991) Heart rate variability and cardiac autonomic function in men with chronic alcohol dependence. Br Heart J 65:84–88
77. Mandelbrot BB (1983) Geometry of nature. Freeman, Sanfrancisco
78. Marwan N, Wessel N, Meyerfeldt U, Schirdewan A, Kurths J (2002) Recurrence-plot-based measures of complexity and their application to heart-rate-variability data. Phys Rev E 66(2)
79. Muller JE, Morrison J, Stone PH, Rude RE, Rosner B, Roberts R et al (1984) Nifedipine therapy for patients with threatened and acute myocardial infarction: a randomized, double-blind, placebo-controlled comparison. Circulation 69:740–747
80. Nagy E, Orvos H, Bardos G, Molnar P (2000) Gender-related heart rate differences in human neonates. Pediatr Res 47(6):778–780
81. Narayana Dutt D, Krishnan SM (1999) Application of phase space techniques to the analysis of cardiac signals. Proceedings of IEEE EMBS conference, Atlanta, USA
82. Ng TT, Chang SF, Sun Q (2004) Blind detection of photomontage using higher order statistics. In: IEEE international symposium on circuits and systems (ISCAS), Vancouver, Canada
83. Niedermaier O, Smith M, Beightol L et al (1993) Influence of cigarette smoking on human autonomic function. Circulation 88:562–571
84. Nikias CL, Rughuveer MR (1987) Bispectrum estimation: a digital signal processing framework. Proc IEEE 75:869–890
85. Oliver F, Acharya UR, Krishnan SM, Min LC (2004) Analysis of cardiovascular signals using spatial filling index and time-frequency domain. Biomed Online J USA 3:30
86. Owis MI, Abou-Zied AH, Youssef ABM, Kadah YM (2002) Study of features on nonlinear dynamical modeling in ECG arrhythmia detection and classification. IEEE Trans Biomed Eng 49(7):733–736
87. Pagani M, Lombardi F, Guzzetti S et al (1986) Power spectral analysis of heart rate and arterial pressure variabilities as a marker of sympatho-vagal interaction in man and conscious dog. Circ Res 59:178–193
88. Pater C, Compagnone D, Luszick J, Verboom C-N (2003) Effect of Omacor on HRV parameters in patients with recent uncomplicated myocardial infarction—a randomized, parallel group, double-blind, placebo-controlled trial: study design. Curr Control Trials Cardiovasc Med 4(2)
89. Paul SA, James NW, Gareth RC, Petter AS, Colin ER (2002) Finding coordinated atrial activity during ventricular fibrillation using wavelet decomposition. IEEE Eng Med Biol Mag 21(1):58–61
90. Pellizzer AM, Kamen PW, Esler MD et al (2001) Comparative effects of mibefradil and nifedipine gastrointestinal transport system on autonomic function in patients with mild to moderate essential hypertension. J Hypertens 19:279–285
91. Peng CK, Havlin S, Hausdorf JM, Mietus JE, Stanley HE, Goldberger AL (1996) Fractal mechanisms and heart rate dynamics. J Electrocardiol 28(Suppl):59–64
92. Pfeifer MA, Cook D, Brodsky J, Tice D, Reenan A, Swedine S et al (1982) Quantitative evaluation of cardiac parasympathetic activity in normal and diabetic man. Diabetes 3:339–45
93. Pincus SM (1991) Approximate entropy as a measure of system complexity. Proc Natl Acad Sci USA 88:2297–2301
94. Pincus SM, Goldberger AL (1994) Physiological time-series analysis: what does regularity quantify? Am J Physiol 266:1643–1656
95. Pincus SM, Viscarello RR (1992) Approximate entropy: a regularity measure for heart rate analysis. Obstet Gynecol 79:249–55
96. Pinhas I, Toledo E, Aravot D, Akselrod S (2004) Bicoherence analysis of new cardiovasculr spectral components observed in heart-transplant patients: statistical approach for bicoherence thresholding. IEEE Trans Biomed Eng 51:1774–1783
97. Pomeranz B, Macaulay RJB, Caudill MA, Kutz I, Adam D, Kilborn KM, Barger AC, Shannon DC, Cohen RJ, Benson H (1985) Assessment of autonomic function in humans by heart rate spectral analysis. Am J Physiol 248:H151–H153

98. Pope CA III, Eatough DJ, Gold DR, Pang Y, Nielsen KR, Nath P, Verrier RL, Kanner RE (2001) Acute exposure to environmental tobacco smoke and heart rate variability. Environ Health Perspect 109(7):711–716
99. Radhakrishna Rao KA, Vikram Kumar Yergani, Narayana Dutt D, Vedavathy TS (2001) Characterizing chaos in heart rate variability time series of panic disorder patients. In: Proceedings of ICBME Biovision. Bangalore, India, pp 163–167
100. Ramaekers D, Ector H, Aubert AE, Rubens A, van de Werf F (1993) Heart rate variability and heart rate in healthy volunteers: Is the female autonomous nervous system cardioprotective? Eur Heart J 19:1334–1341
101. Rao RM, Bopardikar AS (1998) Wavelet transforms introduction to theory and applications. Addison Wesley, Longman Inc, Reading, MA
102. Richman JS, Moorman JR (2000) Physiological time-series analysis using approximate entropy and sample entropy. Am J Physiol Heart Circ Physiol 278:H2039–H2049
103. Richman JS, Randall MJ (2000) Physiological time-series analysis using approximate entropy and sample entropy. Am J Physiol Heart Circ Physiol 278:H2039–H2049
104. Roche F, Pichot V, Sforza E, Court-Fortune I, Duverney D, Costes F, Garet M, Barthélémy J-C (2003) Predicting sleep apnoea syndrome from heart period: a time-frequency wavelet analysis. Eur Respir J 22:937–942
105. Rosenstien M, Colins JJ, De Luca CJ (1993) A practical method for calculating largest Lyapunov exponents from small data sets. Physica D 65:117–134
106. Rossinin J, Vitasalo M, Partanen J et al (1997) Effects of acute alcohol ingestion on heart rate variability in patients with documented coronary artery disease and stable angina pectoris. Am J Cardiol 79:487–491
107. Rother M, Zwiener U, Witte H, Eiselt M, Frenzel J (1988) Objective characterization and differentiation of sleep states in healthy newborns and newborns-at-risk by spectral analysis of heart rate and respiration rhythms. Acta Physiol Hung 71:383–393
108. Rothschild M, Rothschild A, Pfeifer M (1988) Temporary decrease in cardiac parasympathetic tone after acute myocardial infarction. Am J Cardiol 18:637–639
109. Ryan JM, Howes LG (2000) White coat effect of alcohol. Am J Hypertens, 13:1135–1138
110. Ryan SM, Goldberger AL, Pincus SM, Mietus J, Lipsitz LA (1994) Gender-and age-related differences in heart rate: are women more complex than men. J Am Coll Cardiol 24(7):1700–1707
111. Saul JP (1990) Beat-to-beat variations of heart rate reflect modulation of cardiac autonomic outflow. News Physiol Sci 5:32–37
112. Saul J, Rea R, Eckberg D, Berger R, Cohen R (1990) Heart rate and muscle sympathetic nerve variability during reflex changes of autonomic activity. Am J Physiol 258:H713–H721
113. Sayar K, Güleç H, Gökçe M, Ak I (2002) Heart rate variability in depressed patients. Bull Clin Psychopharmacol 12(3):130–133
114. Schumacher A (2004) Linear and nonlinear approaches to the analysis of R–R interval variability. Biol Res Nurs 5(3):211–221
115. Schwartz PJ, Priori SG (1990) Sympathetic nervous system and cardiac arrythmias. In: Zipes DP, Jalife J (eds) Cardiac electrophysiology. From cell to bedside. W.B. Saunders, Philadelphia, pp 330–343
116. Schwartz JB, Gibb WJ, Tran T (1991) Aging effects on heart rate variation. J Gerontol 46:M99–M106
117. Schwartz PJ, La Rovere MT, Vanoli E (1992) Autonomic nervous system and sudden cardiac death. Experimental basis and clinical observations for post-myocardial infarction risk stratification. Circulation 85(Suppl I):I77–I91
118. Shimojima H, Tsutsumi T, Yanagisawa F, Komukai M, Zenda N, Higashi Y, Takeyama Y, Okamoto Y (2003) Application of wavelet transform for analysis of QRS complex in intraventricular conduction abnormalities. Int J Bioelectromagn 5(1):279–281
119. Singh JP, Larson MG, O'Donell CJ, Wilson PF, Tsuji H, Lyod-Jones DM, Levy D (2000) Association of hyperglycemia with reduced heart rate variability: the Framingham heart study. Am J Cardiol 86:309–312
120. Task Force of the European Society of Cardiology and North American Society of Pacing and Electrophysiology (1996) Heart rate variability: standards of measurement, physiological interpretation and clinical use. Eur Heart J 17:354–381
121. Theiler J, Eubank S, Longtin A, Galdrikian B, Farmer JD (1992) Testing for nonlinearity in time series: the method of surrogate data. Physica D 58:77–94
122. Togo F, Yamamoto Y (2000) Decreased fractal component of human heart rate variability during non-REM sleep. Am J Physiol Heart Circ Physiol 280:H17–H21
123. Toledo E, Gurevitz O, Hod H, Eldar M, Akselrod S (2003) Wavelet analysis of instantaneous heart rate: a study of autonomic control during thrombolysis. Am J Physiol Regul Integr Comp Physiol 284(4):R1079–R1091
124. Tsai AC, Chiu HW (2002) Relationship between heart rate variability and electrolyte concentration in chronic renal failure patients under hemodialysis. Int J Bioelectromagn 4(2):307–308
125. Tulen JH, Boomsma F, Man in t'veld AJ (1999) Cardiovascular control and plasma catecholamines during restand mental stress: effects of posture. Clin Sc 96:567–576
126. Tulppo MP, Makikallio TH, Takala TES, Seppanen T, Huikuri HV (1996) Quantitative beat-to-beat analysis of heart rate dynamics during exercise. Am J Physiol 271:H244–H252
127. Van Geijn HP, Jongsma HW, de Haan J, Eskes TK, Prechtl HF (1980) Heart rate as an indicator of the behavioral state. Am J Obstet Gynecol 136:1061–1066
128. Van Ravenswaaij CM, Hopman JC, Kollee LA, Van Amen JP, Stoelinga GB, Van Geijn HP (1991) Influences on heart rate variability in spontaneously breathing preterm infants. Early Hum Dev 27:187–205
129. Verlinde D, Beckers F, Ramaekers D, Aubert AE (2001) Wavelet decomposition analysis of heart rate variability in aerobic athletes. Auton Neurosci 90(1–2):138–141
130. Vetterli M (1992) Wavelet and filter banks: theory and design. IEEE Trans Signal Process 40(9):2207–2232
131. Vetterli M, Kovacevic J (1995) Wavelets and subband coding. Prentice-Hall, Englewood Cliffs, NJ
132. Viktor A, Jurij-MAtija K, Roman T et al (2003) Breathing rates and heart rate spectrograms regarding body position in normal subjects. Comput Biol Med 33:259–266
133. Villa MP, Calcagnini G, Pagani J, Paggi B, Massa F, Ronchetti R (2000) Effects of sleep stage and age on short-term heart rate variability during sleep in healthy infants and children. Chest 117:460–466
134. Villareal RP, Liu BC, Massumi A (2002) Heart rate variability and cardiovascular mortality. Curr Atheroscler Rep 4(2):120–127
135. Weise F, Heydenreich F, Kropf S, Krell D (1990) Intercorrelation analyses among age, spectral parameters of

heart rate variability and respiration in human volunteers. J Interdiscipl Cycle Res 21:17–24
136. West BJ (2000) Fractal physiology and medicine: studies of nonlinear phenomena in life. Science 1. World Scientific, Singapore
137. Westerhof BE, Gisolf J, Stok WJ, Wesseling KH, Karemaker JM (2004) Time-domain cross-correlation baroreflex sensitivity: performance on the EUROBAVAR data set. J Hypertens 22(7):1259–1263
138. Wharton JM, Coleman RE, Strauss HC (1992) The role of the autonomic nervous system in sudden cardiac death. Trends Cardiovasc Med 2:65–71
139. Wheeler T, Watkins PJ (1973) Cardiac denervation in diabetes. Br Med J 4:584–586
140. Wilson PW, Evans JC (1993) Coronary artery prediction. Am J Hypertens 6:309S–313S
141. Witte H, Putsche P, Eiselt M, Arnold M, Schmidt K (2001) Technique for the quantification of transient quadratic phase couplings between heart rate components. Biomed Tech (Berl) 46:42–49
142. Wolf A, Swift JB, Swinney HL, Vastano JA (1985) Determining Lyapunov exponents from a time series. Physica D 16:285–317
143. Woo MA, Stevenson WG, Moser DK, Trelease RB, Harper RH (1992) Patterns of beat-to-beat heart rate variability in advanced heart failure. Am Heart J 123:704–707
144. Yamasaki Y, Kodama M, Matsuhisa M (1996) Diurnal heart rate variability in healthy subjects: effects of aging and sex differences. Am J Physiol 271:303–310
145. Zeskind PS, Gingras JL (2006) Maternal cigarette-smoking during pregnancy disrupts rhythms in fetal heart rate. J Pediatr Psychol 31(1):5–14
146. Zoccali C, Ciccarelli M, Maggiore Q (1982) Defective reflex control of heart rate in dialysis patients: evidence for an afferent autonomic lesion. Clin Sci 63:285–292